

All-In–All-Out Magnetic Domains: X-Ray Diffraction Imaging and Magnetic Field Control

Samuel Tardif,^{1,*} Soshi Takeshita,¹ Hiroyuki Ohsumi,¹ Jun-ichi Yamaura,² Daisuke Okuyama,³ Zenji Hiroi,⁴ Masaki Takata,^{1,5,6} and Taka-hisa Arima^{1,3,5}

¹RIKEN, SPring-8 Center, Sayo, Hyogo 679-5148, Japan

²MCES, Tokyo Institute of Technology, Kanagawa 226-8503, Japan

³RIKEN, CEMS, Wako, Saitama 351-0198, Japan

⁴ISSP, University of Tokyo, Kashiwa 277-8581, Japan

⁵Department of Advanced Materials Science, University of Tokyo, Kashiwa 277-8561, Japan

⁶JASRI, SPring-8, Sayo, Hyogo 679-5148, Japan

(Received 28 July 2014; revised manuscript received 18 November 2014; published 8 April 2015)

Long-range noncollinear all-in–all-out magnetic order has been directly observed for the first time in real space in the pyrochlore $\text{Cd}_2\text{Os}_2\text{O}_7$ using resonant magnetic microdiffraction at the Os L_3 edge. Two different antiferromagnetic domains related by time-reversal symmetry could be distinguished and have been mapped within the same single crystal. The two types of domains are akin to magnetic twins and were expected—yet unobserved so far—in the all-in–all-out model. Even though the magnetic domains are antiferromagnetic, we show that their distribution can be controlled using a magnetic field-cooling procedure.

DOI: 10.1103/PhysRevLett.114.147205

PACS numbers: 75.60.Ch, 75.25.-j, 75.50.Ee, 78.70.Ck

Low-connectivity lattices—such as the pyrochlore lattice (a three-dimensional network of tetrahedra joined by their vertices)—have proven to be rich hosts for new physics. For example, magnetic monopoles and Dirac strings have recently been reported in the so-called spin-ice configuration [1], i.e., when two of the four magnetic moments sitting at the vertices point toward the center of each tetrahedron while the other two moments point away from it (2-in–2-out) in a pyrochlore lattice [2,3]. When all the four magnetic moments point simultaneously either toward the center of the tetrahedron or away from it, i.e., in the so-called all-in–all-out (AIAO) order, the frustration is lifted and only two magnetic configurations exist in the ground state: all-in–all-out and all-out–all-in (AOAI). These two configurations are not equivalent and are related by time-reversal symmetry, as illustrated in Figs. 1(a) and 1(b). Similar AIAO configurations and relevant domain wall spin dynamics have been studied in the distorted kagome lattice, a two-dimensional analog of the pyrochlore lattice [4]. The AIAO order is particularly interesting in many respects in $5d$ transition metal oxides pyrochlores: the combination of the time-reversal symmetry breaking with strong spin-orbit coupling (due to the heavy magnetic element) and electron-electron correlations [evidenced by a metal-insulator transition (MIT)] would be key ingredients to observe the predicted Weyl semimetal state [5]. Furthermore, the two time-reversal symmetric configurations can be seen as twins in a zinc-blende crystal of magnetic monopoles, or as differently oriented realizations of face-centered crystals of elementary magnetic Skyrmions [Fig. 1(c)] [6]. Finally, the AIAO

order is equivalent to a Moessner pseudoferrimagnet [7] and each configuration can be described in terms of pseudo-orientation (all-in–all-out and all-out–all-in being opposite pseudo-orientations). Domains with opposite pseudo-orientations are expected to display time-reversal odd magnetic properties, such as opposite parabolic

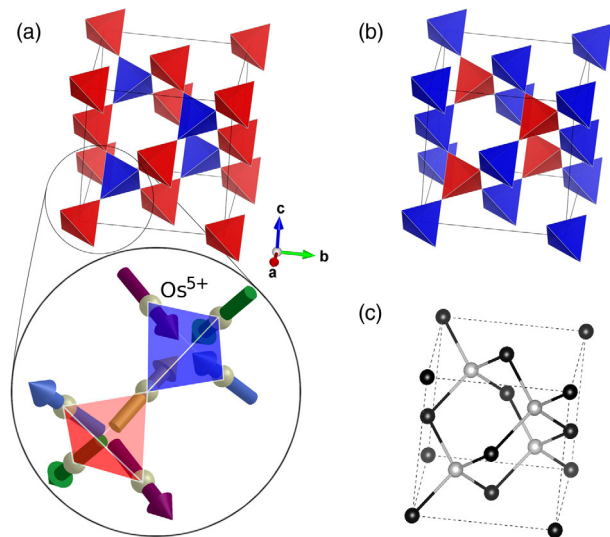


FIG. 1 (color online). (a) All-in–all-out and (b) all-out–all-in magnetic order on the pyrochlore lattice, both configurations are time-reversal symmetric of each other. All Os spins are located at the vertices of the tetrahedra and point either towards the center of the blue (dark gray) tetrahedra or away from the center of the red (light gray) tetrahedra, as shown in the magnified region. (c) Equivalent zinc-blende lattice.

magnetization curves, or opposite linear magnetostriction, magnetocapacitance, and piezomagnetic effect [8]. Probing the magnetic state-dependent physical properties would therefore be highly desirable. In this Letter we tackle the two obstacles in the way of such measurements: (i) the ability to locally distinguish all-in–all-out from all-out–all-in in order to match the local physical properties with the local magnetic orientation, and (ii) the ability to control the local magnetic order.

We propose here to use polarized resonant x-ray micro-diffraction to distinguish between the two possible realizations of the AIAO order (all-in–all-out and all-out–all-in), i.e., to measure experimentally the local pseudo-orientation. As a demonstration, we imaged simultaneously the two types of magnetic domains in $\text{Cd}_2\text{Os}_2\text{O}_7$ single crystals and report on a way to control their distribution. The pyrochlore $\text{Cd}_2\text{Os}_2\text{O}_7$ is highly suited to investigate the properties of the AIAO order since the magnetic transition temperature is relatively high ($T_N = 225$ K). This temperature also corresponds to a continuous MIT [9]. The exact nature of the MIT and the closely related magnetic order of the low temperature insulating phase have recently been the focus of much interest [10–17]. Using symmetry considerations and resonant x-ray diffraction, Yamaura *et al.* recently showed that the spins on the $5d^3\text{Os}^{5+}$ ions order according to the AIAO rule in the low temperature phase [18], and this picture was further supported by various *ab initio* calculations [19].

Since x-ray diffraction can be site, element, and electronic transition specific, it usually allows one to determine the local absolute structural chirality [20–22], local magnetic order [23–25], or local magnetic chirality [26], while circumventing the technical limitations of neutron scattering (nonlocal probe and limited by strong absorbers like Cd) or Lorentz transmission electron microscopy (requiring ultrathin slabs). In order to distinguish the all-in–all-out magnetic order from the all-out–all-in magnetic order, we made use of the interference between the resonant magnetic and resonant nonmagnetic terms of the structure factor. The polarization dependence of the resonant part of the structure factor of the space group-forbidden $004n + 2$ reflections can be written as a sum of two 2×2 matrices between the conventional (σ, π) and (σ', π') bases:

$$F^{(004n+2)} = F_{\text{ATS}} \begin{vmatrix} \sin 2\psi & \sin \theta \cos 2\psi \\ -\sin \theta \cos 2\psi & \sin^2 \theta \sin 2\psi \end{vmatrix} + F_m \begin{vmatrix} 0 & i \sin \theta \\ i \sin \theta & 0 \end{vmatrix}, \quad (1)$$

where F_{ATS} represent the nonmagnetic term, related to the anisotropic tensor susceptibility (ATS) [27], F_m is the magnetic term, related to the magnetic order [28], θ is the Bragg angle, and ψ is the azimuth angle, defined as the angle around the scattering vector such that $\psi = 0$

when [100] is parallel to $\mathbf{k}_i + \mathbf{k}_f$, where \mathbf{k}_i and \mathbf{k}_f are the incident and diffracted wave vector, respectively. As previously noted by Yamaura *et al.* [18], in the special experimental condition where $\psi = 45^\circ$, the scattering plane is parallel to the $(1\bar{1}0)$ plane (i.e., the mirror plane broken by the AIAO order) and the off-diagonal components of the ATS vanish. In this condition, the intensity I^\pm scattered from an incoming beam with the elliptical polarization $\varepsilon^+ = (\sigma_0^+, \pi_0^+)$ or $\varepsilon^- = (\sigma_0^-, \pi_0^-)$ is respectively proportional to

$$I^\pm \propto \|\sigma_0^\pm F_{\text{ATS}} + i\pi_0^\pm \sin \theta F_m\|^2 + \|i\sigma_0^\pm \sin \theta F_m + \pi_0^\pm \sin^2 \theta F_{\text{ATS}}\|^2. \quad (2)$$

We define the flipping ratio (FR) as the contrast in diffraction of an x-ray beam for two opposite handednesses:

$$\text{FR} = \frac{I^+ - I^-}{I^+ + I^-}. \quad (3)$$

In the particular case of circular polarized light (right handed and left handed), the polarization is conventionally described by $(\sigma_0^+, \pi_0^+) = (1, -i)$, $(\sigma_0^-, \pi_0^-) = (1, i)$, respectively. Accordingly, the FR is explicitly given by

$$\text{FR} = \frac{2r \cos \phi \sin \theta (1 - \sin^2 \theta)}{r^2 (1 + \sin^4 \theta) + 2\sin^2 \theta}, \quad (4)$$

where $r = |F_{\text{ATS}}|/|F_m|$ and ϕ is the phase difference between F_{ATS} and F_m . Let us now look closely at the resonant terms: we note that the magnetic structure factor $F_m(\mathbf{Q})$ is proportional to $\mathbf{M}(\mathbf{Q})$, the \mathbf{Q} Fourier component of the Fourier transform of the magnetization $\mathbf{m}(\mathbf{r})$ [29]. At $\mathbf{Q} = 004n + 2$, the sign of $\mathbf{M}(\mathbf{Q})$ is opposite in AIAO and AOAI domains. On the contrary, $F_{\text{ATS}}(\mathbf{Q})$ is only dependent on the local anisotropy, which is the same for both AIAO and AOAI domains; therefore, its sign is constant. As a result, ϕ takes the values of 0 or π ; i.e., the sign of the FR is opposite in opposite types of domains:

$$\text{FR}_{\text{AIAO}} = -\text{FR}_{\text{AOAI}}. \quad (5)$$

The FR can be calculated from successive measurements of the diffracted intensity of the right-handed and left-handed circular polarized x ray and used to distinguish the local magnetic pseudo-orientation.

We performed the FR measurements in high-quality $\text{Cd}_2\text{Os}_2\text{O}_7$ single crystals, as described in Ref. [18]. The measurements were performed at the Os L_3 absorption edges (10.871 keV) and carried out on a magnetic diffraction setup (high resolution in reciprocal space) and on a microdiffraction setup (high resolution in real space), respectively, in experimental hutch 1 and 4 of beam line BL19LXU at the SPring-8 synchrotron radiation source [31].

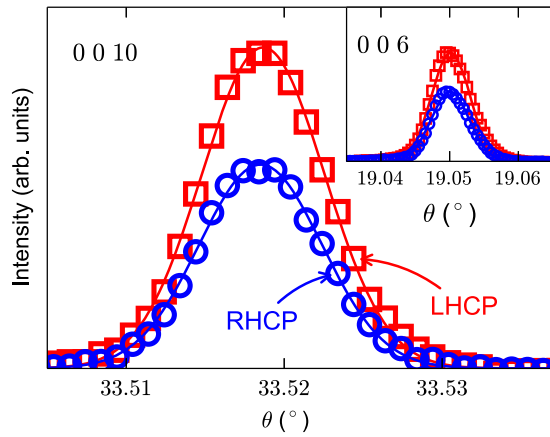


FIG. 2 (color online). Profiles of the forbidden 0010 reflection at the Os L_3 edge (10.871 keV) and at 10 K in the case of left-handed (LHCP) and right-handed (RHCP) circular polarized incident beam. The inset shows the same measurement at the 006 reflection.

After cooling the sample in a magnetic field along a $\langle 111 \rangle$ direction through the ordering temperature down to 10 K, the resonant magnetic x-ray diffraction was measured on the magnetic diffraction setup at space group-forbidden

0010 and 006 reflections for an incident x-ray beam with either left-handed circular polarization or right-handed circular polarization, as shown in Fig. 2. After correction from the incident intensity, a large difference was observed, amounting to a FR of about 22%. The sign of the FR was the same for both the 0010 and the 006 reflections, which is consistent with the observation of either a single all-in-all-out (or all-out-all-in) domain or a strongly unbalanced population of all-in-all-out and all-out-all-in domains.

The local pseudo-orientation of the AIAO and AOAI domains was investigated with submicron resolution on the x-ray microdiffraction setup. The typical results of a mapping experiment with a probe size of $500 \times 500 \text{ nm}^2$ at the 0010 magnetic reflection and $T = 100 \text{ K}$ are shown in Fig. 3(a). The measurement goes over the center (001) facet and the adjacent $\{111\}$ facets of the $\text{Cd}_2\text{Os}_2\text{O}_7$ crystal. In order to be able to compare the magnetic domain maps on different facets of the sample, we corrected the measured maps assuming a slightly misaligned ideal crystal, outlined in Fig. 3(a). In Figs. 3(a)–3(c), one can see that in that configuration the center (001) facet is a single domain with negative FR, while several magnetic domains and domain walls (DW) can be observed on the top and bottom $\{111\}$ facets along high symmetry

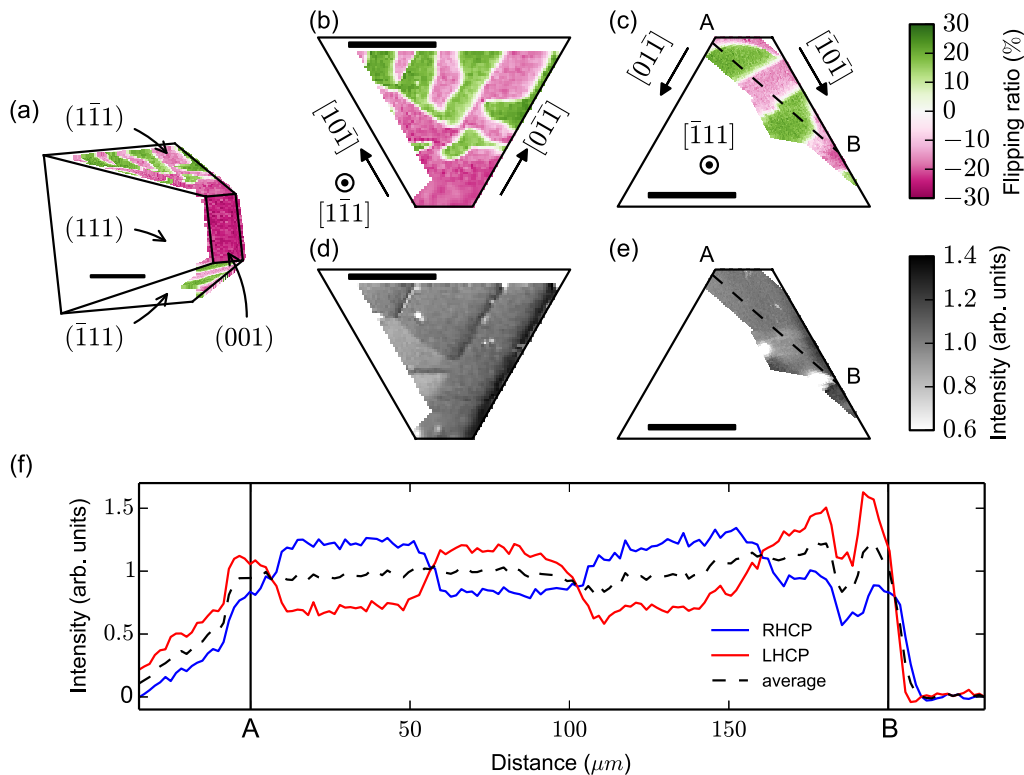


FIG. 3 (color online). (a) FR map at the 0010 reflection, as measured experimentally by rastering the sample in a plane perpendicular to the scattering vector. The ideal crystal is outlined and the orientation of the facets is shown. Opposite signs of the FR indicate opposite pseudo-orientations of the magnetic domains (AIAO versus AOAI). (b),(c) FR maps and (d),(e) normalized intensity on the top ($\bar{1}\bar{1}1$) and bottom ($1\bar{1}\bar{1}$) facets after correction of the projection, respectively. The intensity is normalized to the average value on each facet to outline the deviation from the average structure. All scale bars are $100 \mu\text{m}$ across. (f) Line scan across the bottom ($1\bar{1}\bar{1}$) facet, indicated by the AB dashed line in (c),(e), for both right- and left-handed circular polarization and their average.

orientations. Both top and bottom $\{111\}$ facets show a striplike structure with a typical size in the range of a few tens of micrometers [Figs. 3(b) and 3(c)], much larger than that observed, e.g., in kagome quinternary oxalate compounds [4]. Some preferential orientations of the intersections of the DW with the facets are observed, e.g., $[011]$, $[21\bar{1}]$, $[110]$, $[1\bar{1}\bar{2}]$, $[121]$, and $[10\bar{1}]$ on the top $(1\bar{1}1)$ facet and $[12\bar{1}]$, $[011]$, $[211]$, and $[1\bar{1}2]$ on the bottom $(\bar{1}11)$ facet. Some orientations ($[011]$, $[21\bar{1}]$) are correlated with the distribution of the average intensity, as can be seen by comparing Figs. 3(b) and 3(d). This indicates that in those cases the local magnetic domain structure is probably pinned by crystal defects. The other DW seem to occur at places where the crystal quality is homogeneous, as seen in Figs. 3(c) and 3(e), and further illustrated in Fig. 3(f) where a line scan across the bottom facet shows the alternation of positive and negative FR domains while the average intensity remains constant. We note that only two groups of equivalent DW planes could explain all the orientations of the intersections with the top and bottom facets simultaneously: the “113” group $\{[(113), (1\bar{1}\bar{3}), (1\bar{1}\bar{3}), (\bar{1}13)]\}$ and circular hkl permutations] and the “011” group $\{[(011), (01\bar{1})]\}$ and circular hkl permutations]. The frustration is lower in the 113 group than in the 011 group since there are, respectively, 1 and 4 frustrated moments per unit cell at the DW position [29]. As a result, we would expect the 113 group to be more energetically favorable. However, only the 011 group can account for the $[100]$ orientation observed in Fig. 4(c), which makes it a more likely candidate for the DW orientation. The existence of magnetic DW can explain particular features common to several AIAO magnets, i.e., the finite conductivity at $T = 0$, attributed to transport along the DW, and the nonzero remnant magnetization below T_N [32]. As also suggested in Ref. [4] and consistent with our results, the latter is most likely due to magnetic ordering along the DW.

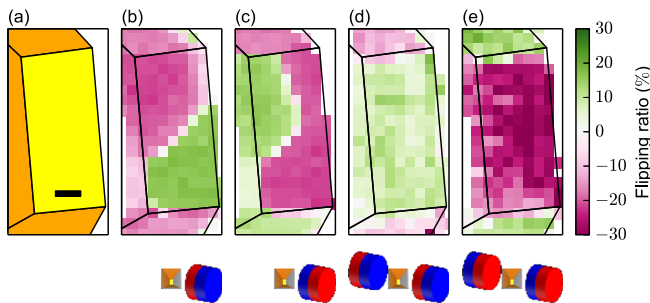


FIG. 4 (color online). (a) Sketch of the sample view in the geometry used, the central rectangle is the (001) facet. The scale bar is $25 \mu\text{m}$ across. (b)–(e) Maps of the flipping ratio across the sample at the 0010 reflection at 100 K for different field-cooling conditions, as sketched in the lower panels. The north pole of the cylindrical permanent magnets is indicated in red (light gray), the magnetic field at the surface of the magnets is 0.4 T. The surface of the magnet is also parallel to the $(\bar{1}\bar{1}1)$ facet, indicated in light gray in the sketch.

In order to assess in more detail the domain reversal observed previously, we performed the same mapping experiment after cooling the sample in a magnetic field. The magnetic domain distributions for different field-cooling configurations are displayed in Figs. 4(b)–4(e), while the outline of the corresponding ideal crystal is shown in Fig. 4(a). In all cases the field was oriented along the $\pm[\bar{1}\bar{1}1]$ direction in the diffraction plane. One can see that for each pair of configurations, reversing the orientation of the magnetic field applied during cooling results in a reversal of the magnetic domain distribution. In the case of the single magnet [Figs. 4(b) and 4(c)], there exists a DW across the center of the (001) facet, oriented along the $[100]$ direction. Upon reversed magnetic field cooling, the domain distribution is reversed over most of the imaged area and the interface retains the same position while the upper right-hand part of the image still remains with the same orientation. The possible origin of this asymmetry is the low reproducibility, homogeneity, and/or magnetic field strength of the single magnet cooling procedure and the pinning of the DW by some crystalline defects. Using a two-magnet configuration yields a different domain distribution with single domains of opposite orientation over the (001) facet and the top $(1\bar{1}1)$ and bottom $(\bar{1}11)$ facets, respectively. Moreover, reversing the more homogeneous cooling field symmetrically reverses the domain distribution over all the imaged area [Figs. 4(d) and 4(e)], demonstrating the reversibility of the procedure.

The magnetic field control of the orientation of antiferromagnetic domains was initially observed by Brown *et al.* in Cr_2O_3 , and it was speculated that this effect was due to defects within the crystal [33]. In $\text{Cd}_2\text{Os}_2\text{O}_7$, the possible origins of the magnetic field control of the AIAO and AOAI domains lie in the domain-dependent magnetic properties described by Arima [8]. To the first order, any small strain that could be induced during the cooling independently of the applied magnetic field (for example, due to the thermal expansion mismatch with the sample holder) will lower the free energy of one of the two pseudo-orientations with respect to the other, in a given orientation of the applied magnetic field. Reversing the magnetic field during cooling will in turn favor the opposite pseudo-orientation. To the second order, the magnetization possesses a nonlinear (parabolic) component, the sign of which is dependent on the pseudo-orientation; i.e., opposite pseudo-orientations will be favored in opposite applied magnetic field. Furthermore, we also suggest that $\{111\}$ surfaces may play a role. On such surfaces, the absence of the fourth Os ion in the tetrahedra results in uncompensated magnetic moments and one can expect a ferromagnetic order of the net magnetic moments on a perfect $\{111\}$ surface, perpendicular to the surface. It is possible that these uncompensated moments couple to the cooling field and set the orientation of the underlying all-in–all-out magnetic order during the cooldown. As a result, the

ability to control the pseudo-orientation paves the way for the study of the magnetic domain-dependent properties, e.g., in the case of (111)-oriented thin films.

In summary, we observed the long-range all-in–all-out magnetic order in the insulating phase of the pyrochlore $\text{Cd}_2\text{Os}_2\text{O}_7$ using polarized resonant magnetic x-ray diffraction. In particular, all-in–all-out magnetic domains could be distinguished from all-out–all-in domains according to the sign of the flipping ratio of left- and right-handed circularly polarized x-ray diffraction. Both types of domains were shown to coexist in single crystals, with sizes in the range of a few tens of microns. Additionally, the pseudo-orientation of the domains could be easily controlled by a simple magnetic field-cooling procedure, consistent with theoretical predictions in the AIAO model. The experimental techniques to image and control the local all-in–all-out order that we describe here are not limited to the particular $\text{Cd}_2\text{Os}_2\text{O}_7$ compound, but may further be applied to any all-in–all-out-type pyrochlores.

This work was funded by the Funding Program for World Leading Innovative R&D on Science and Technology (FIRST) project “Quantum Science on Strong Correlation” (QS2C). Experiments were performed under proposal 20130074 for the RIKEN beam lines at SPring-8. We acknowledge H. Kodera and Y. Hattori for technical assistance during the preparation of the experiments, as well as the staff of BL19LXU at SPring-8 for expert support. We also thank S. Tsujiuchi and N. Torimoto for their help during the experiments at BL19LXU.

*Present address: CEA-Grenoble/INAC/SP2M/NRS, 17 rue des Martyrs, F-38054 Grenoble, France.
samuel.tardif@gmail.com

- [1] D. J. P. Morris *et al.*, *Science* **326**, 411 (2009); T. Fennell, P. P. Deen, A. R. Wildes, K. Schmalzl, D. Prabhakaran, A. T. Boothroyd, R. J. Aldus, D. F. McMorrow, and S. T. Bramwell, *Science* **326**, 415 (2009).
- [2] S. T. Bramwell and M. J. P. Gingras, *Science* **294**, 1495 (2001).
- [3] *Introduction to Frustrated Magnetism: Materials, Experiments, Theory*, edited by C. Lacroix, P. Mendels, and F. Mila (Springer, Berlin, 2011).
- [4] E. Lhotel *et al.*, *Phys. Rev. Lett.* **107**, 257205 (2011).
- [5] X. Wan, A. M. Turner, A. Vishwanath, and S. Y. Savrasov, *Phys. Rev. B* **83**, 205101 (2011).
- [6] X. Z. Yu, Y. Onose, N. Kanazawa, J. H. Park, J. H. Han, Y. Matsui, N. Nagaosa, and Y. Tokura, *Nature (London)* **465**, 901 (2010).
- [7] R. Moessner, *Phys. Rev. B* **57**, R5587 (1998).
- [8] T.-h. Arima, *J. Phys. Soc. Jpn.* **82**, 013705 (2013).
- [9] A. Sleight, J. Gillson, J. Weiher, and W. Bindloss, *Solid State Commun.* **14**, 357 (1974).
- [10] D. Mandrus, J. Thompson, R. Gaal, L. Forro, J. Bryan, B. Chakoumakos, L. Woods, B. Sales, R. Fishman, and V. Keppens, *Phys. Rev. B* **63**, 195104 (2001).
- [11] J. Reading and M. T. Weller, *J. Mater. Chem.* **11**, 2373 (2001).
- [12] D. J. Singh, P. Blaha, K. Schwarz, and J. O. Sofo, *Phys. Rev. B* **65**, 155109 (2002).
- [13] W. J. Padilla, D. Mandrus, and D. N. Basov, *Phys. Rev. B* **66**, 035120 (2002).
- [14] H. Harima, *J. Phys. Chem. Solids* **63**, 1035 (2002).
- [15] A. Koda, R. Kadono, K. Ohishi, S. R. Saha, W. Higemoto, S. Yonezawa, Y. Muraoka, and Z. Hiroi, *J. Phys. Soc. Jpn.* **76**, 063703 (2007).
- [16] G.-W. Chern and C. D. Batista, *Phys. Rev. Lett.* **107**, 186403 (2011).
- [17] Y. H. Matsuda, J. L. Her, S. Michimura, T. Inami, M. Suzuki, N. Kawamura, M. Mizumaki, K. Kindo, J. Yamamura, and Z. Hiroi, *Phys. Rev. B* **84**, 174431 (2011).
- [18] J. Yamaura *et al.*, *Phys. Rev. Lett.* **108**, 247205 (2012).
- [19] H. Shinaoka, T. Miyake, and S. Ishibashi, *Phys. Rev. Lett.* **108**, 247204 (2012); N. A. Bogdanov, R. Maurice, I. Rousochatzakis, J. van den Brink, and L. Hozoi, *Phys. Rev. Lett.* **110**, 127206 (2013).
- [20] J. M. Bijvoet, A. F. Peerdeman, and A. J. van Bommel, *Nature (London)* **168**, 271 (1951).
- [21] Y. Tanaka, S. P. Collins, S. W. Lovesey, M. Matsumami, T. Moriwaki, and S. Shin, *J. Phys. Condens. Matter* **22**, 122201 (2010).
- [22] H. Ohsumi, A. Tokuda, S. Takeshita, M. Takata, M. Suzuki, N. Kawamura, Y. Kousaka, J. Akimitsu, and T.-h. Arima, *Angew. Chem., Int. Ed. Engl.* **52**, 8718 (2013).
- [23] J. C. Lang, D. R. Lee, D. Haskel, and G. Srajer, *J. Appl. Phys.* **95**, 6537 (2004).
- [24] J. W. Kim, A. Kreyssig, L. Tan, D. Wermeille, S. L. Budko, P. C. Canfield, and A. I. Goldman, *Appl. Phys. Lett.* **87**, 202505 (2005).
- [25] P. G. Evans and E. D. Isaacs, *J. Phys. D* **39**, R245 (2006).
- [26] Y. Hiraoka, Y. Tanaka, T. Kojima, Y. Takata, M. Oura, Y. Senba, H. Ohashi, Y. Wakabayashi, S. Shin, and T. Kimura, *Phys. Rev. B* **84**, 064418 (2011).
- [27] V. E. Dmitrienko, *Acta Crystallogr. Sect. A* **39**, 29 (1983).
- [28] S. W. Lovesey and S. P. Collins, *X-Ray Scattering and Absorption by Magnetic Materials* (Clarendon Press, Oxford, 1996).
- [29] See Supplemental Material at <http://link.aps.org/supplemental/10.1103/PhysRevLett.114.147205>, which includes Ref. [30], for a detailed calculation of the polarization dependence of the flipping ratio and a description of the magnetic DW orientations.
- [30] K. Hirano and H. Maruyama, *Jpn. J. Appl. Phys.* **36**, L1272 (1997).
- [31] M. Yabashi *et al.*, *Nucl. Instrum. Methods Phys. Res., Sect. A* **467–468**, 678 (2001); S. Takeshita (to be published).
- [32] Z. Hiroi, J. Yamaura, T. Hirose, I. Nagashima, and Y. Okamoto, *APL Mater.* **3**, 041501 (2015).
- [33] P. J. Brown, *J. Phys. Condens. Matter* **10**, 663 (1998).